

Quantum resonances crossing and survival amplitude for double-well potentials

Andrea Sacchetti ¹

Department of Physics, Informatics and Mathematics, University of Modena and Reggio Emilia, Modena, Italy

ARTICLE INFO

Keywords:

Quantum resonances
Survival amplitude
Avoided crossing

ABSTRACT

In the case of crossings of isolated pairs of quantum resonances for double-well potentials it is possible to observe that, under appropriate conditions, the associated metastable states are equally localized on both wells. This property, together with the fact that the imaginary parts of the two resonances coincide, results in the establishment of an interference phenomenon between the two metastable states that characterizes the time dynamics of certain physical observables. In this way, it is possible to lay the theoretical foundations for the design of a quantum device to assess whether or not the model's parameters assume pre-assigned values.

1. Introduction

In his celebrated paper Berry [1] discusses the crossing scenario that occurs for Hamiltonian systems represented by a 2×2 matrix depending on the some parameters. In the special case of Hermitian systems the real-valued eigenvalues may cross for some values of the parameters. Varying the system's parameters along a closed curve, the eigenvectors undergo a characteristic geometric phase change when the crossing point is encircled. In the non-Hermitian case the two eigenvalues are complex-valued and we can observe a richer scenario because, varying the parameters, typically two different kind of crossings may occur. That is, in one case (named *type I crossing*) the real parts of the complex-valued eigenvalues show an *avoided* crossing while the imaginary parts cross; in the second case (named *type II crossing*) the imaginary parts of the complex-valued eigenvalues show an *avoided* crossing while the real parts cross.

This second type of crossing was described first by Avron [2] for Wannier–Stark ladders of quantum resonances. Later [3] gave a criterion in order to establish the kind of crossing, again in the context of Wannier–Stark ladders of quantum resonances, and then [4,5] extended such a criterion to a more general family of Schrödinger operators studied in the semiclassical limit. More recently [6] explored the avoided crossing scenario and the change of the geometric phase along close paths of the system's parameters in the case of quantum resonances of a double-Dirac's δ potential in a constant (Stark) field.

Let us recall that a quantum resonance, associated to a metastable state, is a complex number whose real part is the energy of the state and its imaginary part is strictly negative and gives the rate of the decay of the state. The mathematical definitions of resonances are typically stationary; e.g.: if the system is associated to a Schrödinger operator H then resonances may be defined as the poles of the meromorphic continuation of the kernel of the resolvent operator $[H - E]^{-1}$. In fact, quantum resonances may be defined by means of several equivalent ways: e.g by means of the Siegert's outgoing conditions or by means of complex dilation methods (see the papers [7–15] and the references therein for a review).

E-mail address: andrea.sacchetti@unimore.it.

¹ Andrea Sacchetti is member of Gruppo Nazionale per la Fisica Matematica of Istituto Nazionale di Alta Matematica (GNFM-INdAM). This work is partially supported by the Next Generation EU - Prin 2022CHELC7 project "Singular Interactions and Effective Models in Mathematical Physics" and the UniMoRe-FIM project "Modelli e metodi della Fisica Matematica".

In their seminal paper [16] García-Calderón and Peierls discussed the possibility to expand the propagator operator $S^t = e^{-itH}$ in terms of the resonances E of the Schrödinger operator $H = -\frac{d^2}{dx^2} + V$, where V is a real-valued potential and $x \in \mathbb{R}$, and their associated metastable states; at this moment, for argument's sake, let us assume the units such that $\hbar = 1$ and $2m = 1$ where m is the mass of the particle. Let $G(x, y; E)$, with $\Im E \geq 0$, be the kernel of the resolvent operator. For $x \neq y$ it is an analytic function and its poles in the *non-physical plane* $\Im E < 0$ are the *resonances* of H . Assuming that V satisfies some suitable assumptions, for instance V is a smooth function with compact support and H has no zero energy resonance, then the kernel $U(x, y; t)$ of the evolution operator S^t is given by [17]

$$U(x, y; t) = \sum_{\text{resonances } E} e^{-itE} \psi_E(x) \psi_E(y) + \sum_{\text{eigenvalues } E} e^{-itE} \psi_E(x) \psi_E(y) + O(t^{-3/2}), \text{ as } t \rightarrow +\infty, \tag{1}$$

where the metastable states ψ_E associated to the resonances E are normalized as $\langle \tilde{\psi}_E, \psi_E \rangle = 1$ and the eigenfunctions (still denoted by ψ_E) associated to the real-valued eigenvalues E are normalized as usual: $\langle \psi_E, \psi_E \rangle = 1$; by $\langle \cdot, \cdot \rangle$ we denote the usual scalar product in the Hilbert space $L^2(\mathbb{R}, dx)$.

Suppose to consider now the time evolution of a quantum observable; for instance of the survival amplitude defined as

$$\mathcal{A}(t) = \langle \psi_0, S^t \psi_0 \rangle$$

where ψ_0 is the initial (normalized) wavefunction; if H has no eigenvalues then (1) becomes

$$\mathcal{A}(t) = \sum_{\text{resonances } E} c_E e^{-itE} + O(t^{-3/2}), \text{ as } t \rightarrow +\infty, \tag{2}$$

where

$$c_E = \langle \psi_0, \psi_E \rangle \langle \tilde{\psi}_0, \psi_E \rangle. \tag{3}$$

Thus, in absence of stable states the survival amplitude decreases in time and we can observe different kinds of decay:

- for short times, in the so called quadratic Zeno region, the dominant term comes from the quadratic approximation of the exponential [18] ;
- for intermediate times the dominant term comes from the exponentially decay effect associated with sharp resonances (that is with imaginary part small enough: $|\Im E| \ll 1$);
- finally, for long times the dominant term is given by the power-law tail $O(t^{-3/2})$.

We consider now the case where the potential V has a *double-well* shape and the Hamiltonian H has no eigenvalues and it admits only two *sharp* quantum resonances E_1 and E_2 . Then (2) takes the form

$$\mathcal{A}(t) \approx \sum_{j=1}^2 c_{E_j} e^{-itE_j}, \tag{4}$$

for intermediate times, where the coefficients c_{E_j} depend on the initial wavefunctions ψ_0 . Therefore, from (4) we expect that $\mathcal{A}(t)$ exhibits one of the following behaviour:

- $\mathcal{A}(t)$ has a *damped oscillating behaviour* when the imaginary parts of the two resonances E_j are close enough and when the coefficients c_{E_j} are both not too small (in absolute value). In this case an interference effect is triggered and $\mathcal{A}(t)$ has a *pseudo-period* given by $T = 2\pi/\omega$, where $\omega = |\Re E_2 - \Re E_1|$;
- $\mathcal{A}(t)$ has an *exponential decay behaviour without significant oscillations* when the imaginary parts of the two resonances E_j are quite different from each other or when one of the two coefficients c_{E_j} is very small; indeed, for example, if $|\Im E_1| \ll |\Im E_2|$ or if $c_{E_2} \approx 0$ then $\mathcal{A}(t) \approx c_{E_1} e^{-itE_1}$ has a purely exponentially decreasing behaviour.

In this paper, in order to investigate this fact with numerical experiments, we consider a one-dimensional double-well potential with two square wells. In fact, in this explicit model numerical investigation becomes relatively easy; furthermore, it is a typical potential in heterostructures and thus it can be a prototype for a proposal of quantum devices. Eventually, we consider also theoretical investigations for more generic double-well potentials in the semiclassical limit.

In the case of the potential plotted in Fig. 1 – full line – we say that it is a *stable double-well potential* and the Schrödinger operator has discrete eigenvalues in the interval $(\alpha, 0)$, where $\alpha < 0$. When we vary the model's parameters then we can make the eigenvalues closer and closer; since in dimension one the eigenvalues are always non degenerate then they cannot cross and an avoided crossing picture occurs.

On the other hand, in the case of an *unstable double-well potential* (see Fig. 1 - broken line) then there are no eigenvalues but quantum resonances, and when we vary the model's parameters they can *cross*; in particular the two different kinds of resonances crossing introduced above may occur: type *I* or type *II* crossings. Only in exceptional cases, for very particular values of the model's parameters, the exact intersection of the two resonances may occur.

By means of the new results obtained in this paper we can emphasize that the occurrence of quantum resonance crossing of type *I* is related with a further fact: at the crossing point the two metastable states ψ_{E_1} and ψ_{E_2} associated to the quantum resonances E_1 and E_2 are substantially equally supported within both wells. This result is well known in the case of eigenvectors associated to

real-valued eigenvalues for symmetric stable double-well potentials, but the fact that this property holds true even for asymmetrical stable or unstable double-well potentials is rather new. In fact, we already know that when we broke the symmetry in a stable double-well potential then the wavefunctions suddenly localize themselves on just one of the two wells [19,20]; on the contrary, as far as we know, it is a rather new fact that we can tune the stable/unstable asymmetrical double-well potential's parameters in such a way that the two eigenvalues/resonances (almost) cross and the associated wavefunctions/metastable states are equally supported within both wells.

Therefore, when the initial states ψ_0 is prepared on just one well then, according with (4), we can see an oscillating behaviour of the survival probability only in the occurrence of quantum resonance crossing of type *I*. Indeed, for such a kind of crossing then $|c_{E_1}| \approx |c_{E_2}|$ because the two metastable states are equally supported within both wells; on the other hand $c_{E_1} \approx 0$ or $c_{E_2} \approx 0$ in the case of quantum crossing resonances of type *II* or, in the case of quantum resonances crossing of type *I*, when we are sufficiently far from the crossing point.

The paper is organized as follows.

In Section 2 we introduce the one-dimensional double-well potential with square wells, it is physically inspired from heterostructure devices studied by means of the envelope function approximation.

In Section 3 we discuss the spectral properties of the *stable* double-well model. The results described in Section 3.1 in the case of symmetric stable double-well potentials are basically well known; however, it is useful to take them up again in view of the discussion of subsequent sections where new results are presented. In fact, we will show that the eigenvectors are substantially supported within both wells when we are close to a crossing point even in the case of asymmetrical double-well potentials. Furthermore, we give a rigorous justification of this fact by collecting some results obtained in the semiclassical limit $\hbar \ll 1$.

In Section 4 we discuss the resonances crossing in the case of an *unstable* double-well model. Also in this case we show that the metastable states are substantially supported within both wells when we are in the type *I* crossing point. Furthermore, also in this case we give a rigorous justification of this fact in the semiclassical limit $\hbar \ll 1$.

In Section 5 we compute the survival amplitude $\mathcal{A}(t)$. In particular, we show that when we are in a neighbourhood of the crossing point of type *I* then it has an oscillating behaviour because of formula (4). Since this formula holds true only in approximate sense we compute the survival amplitude numerically too, by making use of the spectral splitting method (explained in Appendix), in order to numerical validate the use of formula (4).

In Section 6 we close with some comments and the proposal of a design of a quantum sensor.

2. Description of the model

Here, we consider the one-dimensional time-dependent Schrödinger equation

$$\begin{cases} i\hbar \frac{\partial \psi}{\partial \tau} = \mathcal{H}\psi \\ \psi(z, \tau)|_{\tau=0} = \psi_0(z) \end{cases}, \quad \psi(\cdot, \tau) \in L^2(\mathbb{R}, dz), \quad (5)$$

where $\psi_0(z)$ is the initial wave-function; \mathcal{H} denotes the Schrödinger operator

$$\mathcal{H} = -\frac{\hbar^2}{2m} \frac{d^2}{dz^2} + \mathcal{V},$$

formally defined on the Hilbert space $L^2(\mathbb{R}, dz)$, with potential $\mathcal{V}(z)$; \hbar is the Planck's constant and m is the particle's mass.

We assume that the potential \mathcal{V} has a *double-well shape*. For instance, in numerical experiments \mathcal{V} is a *square double-well potential* (see Section 2.1); however, in the semiclassical limit our analysis may be extended to a more general family of potentials, like the *mexican hat potential* (see, e.g. [21] and the references therein).

Furthermore, a one-dimensional *toy* model where the two wells are given by a couple of attractive Dirac's δ [22] has been considered too; in fact, one may extend this model to the case of higher dimension (see [23] for the theoretical treatment of Dirac's δ in any dimension). Finally, we should also mention that one can consider the case where the distance between the two wells vanishes (see [24] for the two-dimensional model, see also the references therein); although this problem may be of some interest in a general theoretical analysis we must underline that the phenomenon of resonances crossing takes place only when the length of the inner barrier is sufficiently large.

If we denote

$$\mathcal{V}_\infty := \liminf_{|z| \rightarrow \infty} \mathcal{V}(z)$$

and \mathcal{V}_\pm the two minimum values of the potential then we speak of

- *stable double-well potential* when \mathcal{V}_+ or \mathcal{V}_- are strictly less than \mathcal{V}_∞ , in this case the discrete spectrum of \mathcal{H} is not empty;
- *unstable double-well potential* when $\mathcal{V}_\infty \leq \min[\mathcal{V}_-, \mathcal{V}_+]$, in this case the discrete spectrum of \mathcal{H} is empty.

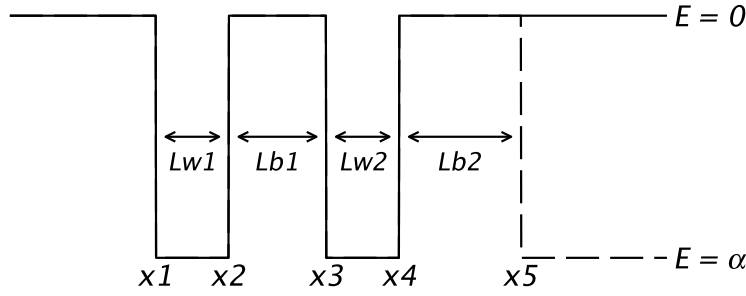


Fig. 1. Full line represents a *stable* double-well potential $V_{\alpha_1, \alpha_2, 0}$ with an *internal* barrier with length L_{b_1} in dimensionless units, and two infinite barriers $(-\infty, x_1)$ and $(x_4, +\infty)$. Broken line represents an *unstable* double-well potential $V_{\alpha_1, \alpha_2, \alpha_3}$ with an *internal* barrier with length L_{b_1} and an *external* one with length L_{b_2} in dimensionless units. For sake of definiteness in the picture we have chosen $\alpha_1 = \alpha_2 = \alpha_3$ and $\alpha < 0$ denotes their common value.

2.1. Heterostructure potential

Square double-well potentials will be considered in numerical experiments; thus we will introduce them in detail. Furthermore, they are useful in order describe the dynamics of electrons in heterostructures (see [25] for a review on heterostructures). For instance, we may consider $GaAs/Ga_rAl_sAs$ heterostructures, where $s \in (0, 1)$ and $r = 1 - s$, with two wells of the kind

$$Ga_rAl_sAs/\ell_{w_1} \cdot GaAs/\ell_{b_1} \cdot Ga_rAl_sAs/\ell_{w_2} \cdot GaAs/Ga_rAl_sAs, \tag{6}$$

The two wells have lengths ℓ_{w_1} and ℓ_{w_2} and the *internal* (or *inner*) barrier has length ℓ_{b_1} . In the envelope function approximation the time independent Schrödinger equation is reduced to a one-dimensional equation where the potential has a stable double-well shape with two square wells (see Fig. 1 – full line – in dimensionless units). We also extend our analysis to the *unstable* double-well model of the kind

$$Ga_rAl_sAs/\ell_{w_1} \cdot GaAs/\ell_{b_1} \cdot Ga_rAl_sAs/\ell_{w_2} \cdot GaAs/\ell_{b_2} \cdot Ga_rAl_sAs/GaAs, \tag{7}$$

where ℓ_{b_2} is the length of the *external* (or *outer*) barrier; in such a case the shape of the one-dimensional potential in the envelope function approximation is represented in Fig. 1 – broken line – in dimensionless units.

With more details, in the envelope function approximation the time independent Schrödinger equation takes the form

$$H\psi = \mathcal{E}\psi \quad \text{where} \quad H = -\frac{\hbar^2}{2m} \frac{d^2}{dz^2} + \mathcal{V}_{v_1, v_2, v_3}, \quad z \in \mathbb{R}, \tag{8}$$

where m is the *effective* mass of the electron. The potential $\mathcal{V}_{v_1, v_2, v_3}(z)$ is a piecewise constant function of the form

$$\mathcal{V}_{v_1, v_2, v_3}(z) = \begin{cases} 0 & \text{if } z \leq z_1 := 0 \\ v_1 & \text{if } z_1 < z < z_2 := z_1 + \ell_{w_1} \\ 0 & \text{if } z_2 \leq z \leq z_3 := z_2 + \ell_{b_1} \\ v_2 & \text{if } z_3 < z < z_4 := z_3 + \ell_{w_2} \\ 0 & \text{if } z_4 \leq z \leq z_5 := z_4 + \ell_{b_2} \\ v_3 & \text{if } z_5 < z \end{cases}, \quad \text{where } v_1, v_2 < 0 \text{ and } v_3 \leq 0. \tag{9}$$

Thus, the two wells correspond to the intervals (z_1, z_2) and (z_3, z_4) , the internal barrier corresponds to the interval (z_2, z_3) and the external barrier, that is present when $v_3 < 0$, corresponds to the interval (z_4, z_5) . Hereafter, for the sake of definiteness, we have chosen $z_1 = 0$.

Remark 2.1. We underline that this model includes the case where the external barrier has infinite length, i.e. $\ell_{b_2} = +\infty$, by choosing $v_3 = 0$, as in Section 3. Furthermore, we emphasize that in the case of heterostructures of the kind (6) and (7) the potential in the well has the same value, i.e. $v_1 = v_2$; however one can consider, in principle, even cases where $v_1 \neq v_2$ as in Section 3.2.

Remark 2.2. In this paper we consider the simplest case where the effective electron mass in the wells coincides with the one in the barriers and it is given by $m = 0.067m_0$ for $GaAs$ lattices (m_0 is the electron mass) and the matching conditions are of the form

$$\psi(z) \text{ and } \frac{d\psi(z)}{dz} \text{ continuous at } z_n, \quad n = 1, \dots, 5. \tag{10}$$

In fact, such an approximation holds true provided that the parameter $s \in (0, 1)$ is not too large, typically $s \leq 0.3$ (see Fig. 2.17 by [25]). A more refined model is to assume that the effective mass m_w in the wells is different from that m_b in the barriers; that is, if we denote by $\psi_w(z)$, (resp. $\psi_b(z)$), the solution of the time independent Schrödinger equation in the wells (resp. barriers), then the matching conditions satisfy the so-called Ben–Daniel and Duke conditions (see §2.6 by [25])

$$\psi_b(z_n) = \psi_w(z_n) \quad \text{and} \quad \frac{1}{m_b} \frac{d\psi_b(z_n)}{dz} = \frac{1}{m_w} \frac{d\psi_w(z_n)}{dz}, \quad n = 1, \dots, 5. \tag{11}$$

However, in this paper, we do not dwell on the analysis of such matching conditions (11).

2.1.1. Dimensionless units

If we set $z = \lambda x$, where $\lambda = 1 \text{ \AA} = 10^{-10} \text{ m}$ then Eq. (8) takes the dimensionless form

$$H\psi = E\psi \quad \text{where} \quad H = -\frac{d^2\psi}{dx^2} + V_{\alpha_1, \alpha_2, \alpha_3}, \quad x \in \mathbb{R}, \quad (12)$$

where $\mathcal{E} = \lambda E$, $\mathcal{V} = \lambda V$, $A = \frac{\hbar^2}{2m\lambda^2}$, $x_n = z_n/\lambda$, $n = 1, \dots, 5$, and (see Fig. 1)

$$V_{\alpha_1, \alpha_2, \alpha_3}(x) = \begin{cases} 0 & \text{if } x \leq x_1 := 0 \\ \alpha_1 & \text{if } x_1 < x < x_2 \\ 0 & \text{if } x_2 \leq x \leq x_3 \\ \alpha_2 & \text{if } x_3 < x < x_4 \\ 0 & \text{if } x_4 \leq x \leq x_5 \\ \alpha_3 & \text{if } x_5 < x \end{cases} \quad \text{where } \alpha_j = v_j/\Lambda, \quad j = 1, 2, 3. \quad (13)$$

Then, the lengths of the wells and barriers are, in dimensionless units, $L_{w_j} = \lambda^{-1} \ell_{w_j}$ and $L_{b_j} = \lambda^{-1} \ell_{b_j}$, $j = 1, 2$. Furthermore, Eq. (5) becomes

$$\begin{cases} i \frac{\partial \psi}{\partial t} = H\psi, & \text{where } t = \Lambda \tau / \hbar \\ \psi(x, t)|_{t=0} = \psi_0(x) \end{cases}. \quad (14)$$

Remark 2.3. Since $m = 0.067m_0$ for a *GaAs* lattice then

$$A = \frac{\hbar^2}{2m\lambda^2} = 0.110(0) \cdot 10^{-16} \frac{\text{J}^2 \cdot \text{s}^2}{\text{Kg} \cdot \text{m}^2}.$$

Concerning α_j , in the numerical experiments we assume, for the sake of definiteness, that v_j is of the order of some hundreds of meV; for instance, if $v_j = -165 \text{ meV}$ (which corresponds to the case $s \approx 0.2$) then

$$\alpha_j = v_j/\Lambda = -165 \text{ meV}/\Lambda = -0.264(4) \cdot 10^{-2}.$$

3. Stable double-well model

In this Section we discuss at first the spectral properties of the Schrödinger operator H formally defined by (12) on $L^2(\mathbb{R})$, where $\alpha_1, \alpha_2 < 0$ and $\alpha_3 = 0$ (see Fig. 1 - full line); in this case stationary states are admitted and for this reason we denoted this model as *stable double-well model*. In particular, in Section 3.1 we consider the case of stable double-well potentials with $\alpha_1 = \alpha_2$; in Section 3.2 we consider the case where $\alpha_1 \neq \alpha_2$.

In both cases, by varying the model's parameters we show the occurrence of the avoided crossing phenomenon between the two energy levels of the stationary (ground) states. Then, we numerically show that in a neighbourhood of the (avoided) crossing point the associated wavefunctions are equally *supported* within both wells; outside of this neighbourhood it turns out that one of the two wavefunctions is mostly supported within just one of the two wells, while the other wavefunction is mostly supported within the other well.

Eventually, in Section 3.3 we prove that the above result can be explained in the semiclassical limit when \hbar goes to zero, with a full agreement with the outputs of the numerical experiment performed for fixed values of the parameters in a realistic model.

With more details, the spectrum of the Schrödinger operator H , formally defined on $L^2(\mathbb{R})$ as $H = -\frac{d^2}{dx^2} + V_{\alpha_1, \alpha_2, 0}$, is such that $\sigma_{\text{ess}}(H) = [0, +\infty)$, where $\sigma_{\text{ess}}(H)$ is the *essential* spectrum of H . The discrete spectrum of H , that consists of isolated eigenvalues, is contained in the interval $(\alpha, 0)$, $\alpha = \min(\alpha_1, \alpha_2)$, and the eigenvalues and wavefunctions are obtained by assuming the matching conditions

$$\psi(x) \quad \text{and} \quad \frac{d\psi(x)}{dx} \quad \text{continuous at } x_n, \quad n = 1, \dots, 4, \quad (15)$$

and the outgoing conditions

$$\psi(x) \rightarrow 0 \quad \text{when } x \rightarrow \pm\infty.$$

Since we are interested in studying the avoided crossing phenomenon for an isolated doublet of eigenvalues E_1 and E_2 of H , then we look for a general solution to equation $H\psi = E\psi$ for $E \in (\bar{\alpha}, 0)$, $\bar{\alpha} = \max(\alpha_1, \alpha_2) < 0$, given by:

$$\psi(x) = \begin{cases} a \exp(kx) & \text{if } x < x_1 := 0 \\ b \cos(h_1x) + c \sin(h_1x) & \text{if } x_1 < x < x_2 \\ d \exp(kx) + e \exp(-kx) & \text{if } x_2 < x < x_3 \\ f \cos(h_2x) + g \sin(h_2x) & \text{if } x_3 < x < x_4 \\ h \exp(-kx) & \text{if } x_4 < x \end{cases}$$

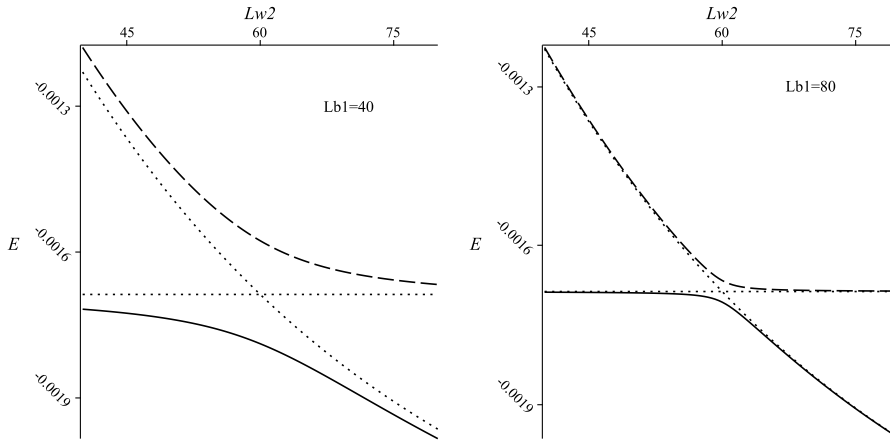


Fig. 2. Here we plot the avoided crossing picture for the two states $E_1 < E_2$ (the ground state E_1 is the full line, E_2 is the broken one) of H when the length L_{w_2} of the second well varies from 40 to 80; since the length L_{w_1} of the first well is 60 then the avoided crossing point is for $L_{w_2} = L_{w_1} = 60$. The length of the barrier is $L_{b_1} = 40$ in the left hand side panel, in the right hand side panel we consider the case of a larger barrier with $L_{b_1} = 80$. The dot lines correspond to the eigenvalues of the two single well operators H_1 and H_2 defined by (16) obtained by filling one of the two wells.

where

$$k = \sqrt{-E} > 0 \quad \text{and} \quad h_j = \sqrt{E - \alpha_j} > 0, \quad j = 1, 2.$$

By choosing the parameters appropriately, the discrete spectrum of H has a doublet of two ground states with energy levels E_1 and E_2 which almost cross each other for some values of the model's parameters.

Here, we consider two different situations. In the first one both wells have the same depth, i.e. $\alpha_1 = \alpha_2$; we refer to this model as a *symmetric stable double-well model*. In the second one the two wells have different depth, i.e. $\alpha_1 \neq \alpha_2$; we refer to this model as a *asymmetrical stable double-well model*.

3.1. Eigenvalues avoided crossing in a symmetric stable double-well model

Here, we consider two numerical experiments with different barrier lengths; we assume that:

- The heterostructure parameter s is chosen such that $\alpha_{1,2} = -0.264(4) \cdot 10^{-2}$ in dimensionless units, furthermore $\alpha_3 = 0$.
- The left hand side well has length $L_{w_1} = 60$ in dimensionless units.
- In the first numerical experiment the barrier has length $L_{b_1} = 40$ in dimensionless units; in the second numerical experiment we consider the case of a larger barrier where $L_{b_1} = 80$ in dimensionless units.
- The value L_{w_2} of the length of the other well runs between 40 to 80 in dimensionless units.

For these values of the model's parameters the discrete spectrum of H has stationary solutions with two ground states with energy levels $E_1 < E_2$ that almost cross each other at $L_{w_2} = L_{w_1}$ because of the symmetry of the potential. We plot the avoided crossing picture in the case where $L_{b_1} = 40$ (see Fig. 2 - left hand side panel); in the case of a larger barrier such that $L_{b_1} = 80$ the avoided crossing picture is plotted in Fig. 2 - right hand side panel. One can observe the typical avoided crossing phenomena: that is when L_{w_2} is close to L_{w_1} the two eigenvalues E_1 and E_2 become closer and closer but they cannot cross because the ground state E_1 is always non-degenerate (in fact, in dimension one all the eigenvalues are non-degenerate). The avoided crossing phenomenon is more evident for larger barriers. In Fig. 2 we also plot – dot lines – the energies of the ground state of the two operators

$$H_1 = -\frac{d^2}{dx^2} + V_{\alpha_1,0,0} \quad \text{and} \quad H_2 = -\frac{d^2}{dx^2} + V_{0,\alpha_2,0} \tag{16}$$

with single well potentials $V_{\alpha_1,0,0}$ and $V_{0,\alpha_2,0}$ obtained by filling one of the two wells.

As a further analysis we estimate how much the normalized wavefunctions ψ_1 and ψ_2 associated to E_1 and E_2 are supported within each of the two wells. In fact, it is well known that in the symmetric case, where $L_{w_1} = L_{w_2}$, the two wavefunctions ψ_1 and ψ_2 respectively are even and odd functions and then they are *equally* supported within both wells. In order to give a measure of how much the wavefunctions are supported within each well let us introduce the following quantities:

$$P_{j,\ell} = \int_{x_1}^{x_2} |\psi_j(x)|^2 dx \quad \text{and} \quad P_{j,r} = \int_{x_3}^{x_4} |\psi_j(x)|^2 dx, \quad j = 1, 2. \tag{17}$$

If one wavefunction, say ψ_1 , is mostly supported within just one well, say the left hand side well $[x_1, x_2]$, then $P_{1,\ell}$ will be close to the value 1 and $P_{1,r}$ to the value zero. On the other side, in correspondence of the crossing point, that is when $L_{w_1} = L_{w_2}$, the two wavefunctions are even and odd functions and then $P_{j,\ell} = P_{j,r} \approx \frac{1}{2}$, $j = 1, 2$.

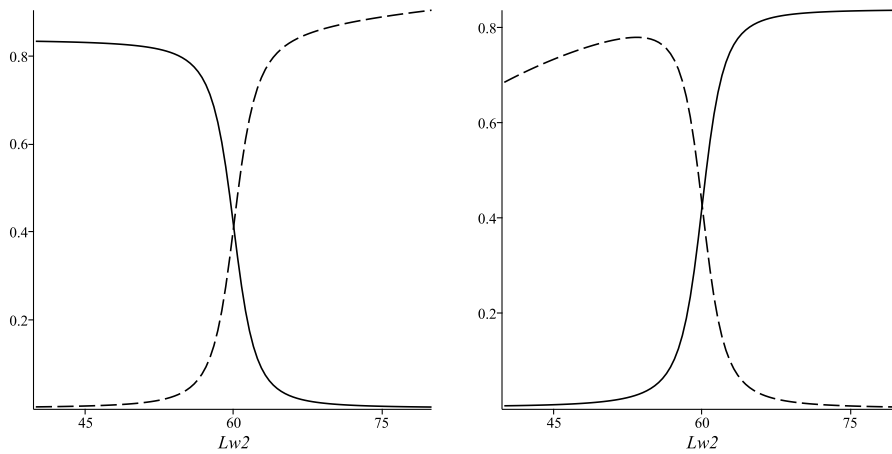


Fig. 3. In the case of $L_{b_1} = 80$ we plot the graphs of the quantities $P_{1,\ell}$ (full line) and $P_{1,r}$ (broken line) in the left hand side panel; in the right hand side panel we plot the graphs of the functions $P_{2,\ell}$ (full line) and $P_{2,r}$ (broken line). When L_{w_2} runs in the interval $[55, 65]$ the well where each wavefunction is mostly supported interchange with the other one.

We have numerically computed the quantities $P_{j,\ell}$ and $P_{j,r}$, $j = 1, 2$, in the case of larger barrier corresponding to $L_{b_1} = 80$; as one can see in Fig. 3 the two wavefunctions are mostly supported within just one of the two wells when we are far from the crossing point (that is when $|L_{w_2} - L_{w_1}| \gtrsim 5$), and

$$P_{j,\ell} \approx P_{j,r} \approx \frac{1}{2}, \quad j = 1, 2,$$

when the model's parameter L_{w_2} is in a neighbourhood of the crossing point. With more details, it turns out that the first wavefunction ψ_1 is mostly supported within the left hand side well $[x_1, x_2]$ when $L_{w_2} < L_{w_1} - 5$, and when L_{w_2} becomes bigger than $L_{w_1} + 5$ then ψ_1 is mostly supported within the other well $[x_3, x_4]$; the opposite situation holds for ψ_2 . On the other hand, when L_{w_2} runs from $L_{w_1} - 5$ to $L_{w_1} + 5$ then the interval where ψ_1 is mostly supported switches from the first well to the second one, and the interval where ψ_2 is supported switches from the second well to the first one. A similar result holds true also when $L_{b_1} = 40$, even if the neighbourhood of the crossing point in which the wavefunctions switch the well where they are supported with the other one is larger of the one observed for $L_{b_1} = 80$; in fact, one can check that the switch of the wells occurs when L_{w_2} runs from $L_{w_1} - 15$ to $L_{w_1} + 15$.

3.2. Eigenvalues avoided crossing in an asymmetrical stable double-well model

From 2 and 3 it turns out that the avoided crossing phenomenon between the two energy levels E_1 and E_2 is connected to the fact that the two associated wavefunctions are, at the crossing point, supported within both wells. In the case of symmetric potentials, where $\alpha_1 = \alpha_2$ and $L_{w_1} = L_{w_2}$, this phenomenon can be explained by means of the fact that the wavefunctions must be even or odd functions and thus $P_{j,\ell} = P_{j,r}$ at the crossing point. The question now is: *what happens in the case of asymmetrical potentials?* Because in dimension one the eigenvalues are always non-degenerate then the avoided crossing phenomenon still occurs even for asymmetrical potentials; but, in principle, its is not clear whether at the crossing point the wavefunctions are still equally supported within both wells like in the case of symmetric potentials. In order to understand what happens we consider now the numerical experiment where:

- $\alpha_1 = -0.264(4) \cdot 10^{-2} < \alpha_2 = -0.2 \cdot 10^{-2}$; hence, we are considering an asymmetrical double-well potential where one well is deeper than the other one;
- $L_{w_1} = 60$;
- $L_{b_1} = 80$;
- L_{w_2} runs in the interval $[110, 150]$.

In a neighbourhood of $L_{w_2} = 130$ we can observe in Fig. 4 an avoided crossing picture between the two energy levels E_1 and E_2 , and the two associated wavefunctions ψ_1 and ψ_2 are supported within both wells; on the contrary, when L_{w_2} has value quite different from the critical value where the avoided crossing phenomenon occurs, that is $|L_{w_2} - 130| \gtrsim 10$, then each wavefunction is mostly supported within just one of the two wells. Hence, also in the case of the asymmetrical stable double-well potential considered we have the same picture already observed in the case of the symmetric stable double-well potential; that is the avoided crossing phenomenon is associated to the interchange of the well where each wavefunction is supported.

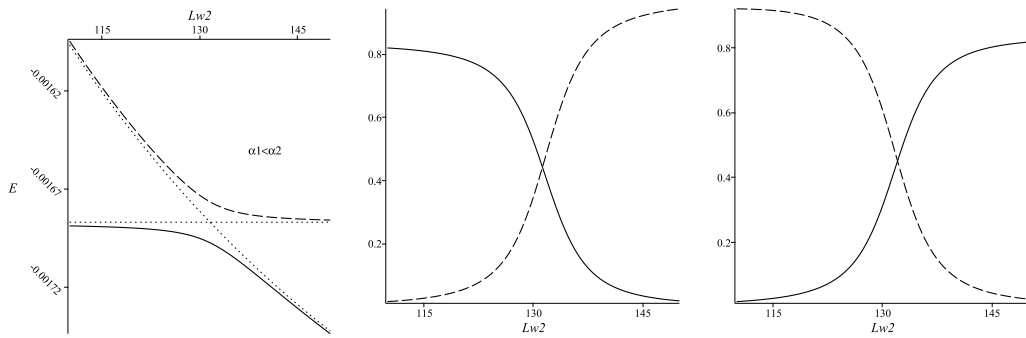


Fig. 4. In the case of asymmetrical double-well where $\alpha_1 < \alpha_2$ the two ground states E_1 (full line) and E_2 (broken line) exhibit in the left hand side panel an avoided crossing scenario in a neighbourhood of the value of Lw_2 for which the two ground states (dot lines) of the single well operators H_1 and H_2 , obtained by filling one of the wells, exactly cross. We also plot the graphs of the quantities $P_{1,l}$ (full line) and $P_{1,r}$ (broken line) – central panel – and of the quantities $P_{2,l}$ (full line) and $P_{2,r}$ (broken line) - right hand side panel.

3.3. Explanation of the avoided crossing picture in the semiclassical limit

From the numerical experiments performed in Sections 3.1 and 3.2 we can conjecture that *in stable double-well models, both symmetric and asymmetrical, the avoided crossing phenomenon of isolated doublets of energy levels is always associated with the interchange of the well where each wavefunction is supported.*

In order to theoretically understand why an avoided crossing scenario occurs for both symmetric and asymmetrical stable double-well potentials and where the associated wavefunctions are mostly supported we make use of the semiclassical results (which means $\hbar \ll 1$) developed by Helffer and Sjöstrand [26,27]. In such a treatment some regularity assumptions on the potential \mathcal{V} are required.

The idea is that the two eigenvalues E_1, E_2 , and the associated wavefunctions ψ_1 and ψ_2 , are connected to the ones of a simple 2×2 symmetric matrix

$$\begin{pmatrix} \mu_1 & \beta \\ \beta & \mu_2 \end{pmatrix} \tag{18}$$

where μ_1 and μ_2 are the ground states of the two single well operators similar to H_1 and H_2 , defined by (16) obtained by filling one of the two well, and where β is a real-valued coupling semiclassical parameter. In fact, the eigenvalues of the matrix (18) are given by

$$\frac{1}{2}(\mu_1 + \mu_2) \pm \frac{1}{2}\sqrt{(\mu_1 - \mu_2)^2 + 4\beta^2}$$

and thus at the crossing point the splitting of the two eigenvalues is given by $|\beta|$.

3.3.1. General setting

We recall some facts by making use of the notation in §4 by [27] and simplifying, as much as possible, the treatment. In this section we denote by $\mathcal{H} = -\frac{\hbar^2}{2m}\Delta + \mathcal{V}$ the Schrödinger operator formally defined on $L^2(\mathbb{R}^d)$ (in our one-dimensional model introduced in Section 2 we have $d = 1$), for argument's sake [27] we assumed that $2m = 1$, if not we simply rescale $\hbar \rightarrow \hbar/\sqrt{2m}$. The potential $\mathcal{V}(z), z \in \mathbb{R}^d$, is assumed to be a regular, i.e. $\mathcal{V} \in C^\infty(\mathbb{R}^d)$, real-valued function such that

$$-\infty < \mathcal{V}_{\min} := \inf_{z \in \mathbb{R}^d} \mathcal{V}(z) < \mathcal{V}_\infty := \liminf_{|z| \rightarrow +\infty} \mathcal{V}(z).$$

Let

$$\mathcal{V}^{-1}(\{\mathcal{V}_{\min}\}) = \{z_j, j = 1, 2, \dots, N\}$$

for some $N \geq 1$. Then for any fixed $\mathcal{V}_{\min} < \mathcal{E} < \mathcal{V}_{\min} + \delta \leq \mathcal{V}_\infty$, for some $\delta > 0$ small enough, let

$$\mathcal{V}^{-1}((-\infty, \mathcal{E}]) = \cup_{j=1}^N U_j$$

where U_j are compact and disjoint sets called *wells* with zero diameter with respect to the Agmon (pseudo-)distance ρ_A defined as follows:

$$\rho_A(z, \zeta; \mathcal{E}) = \inf_\gamma \int_\gamma \sqrt{\max[\mathcal{V} - \mathcal{E}, 0]} ds$$

where γ is any path in \mathbb{R}^d connecting z and ζ . In the case of a double-well potential then $N = 2$ for any \mathcal{E} bigger than the two minimum values of \mathcal{V} . In the following, for argument's sake, we assume that $\mathcal{V}_{\min} < 0$ and we fix $\mathcal{E} = 0$.

Let

$$B_{j,\eta} = \{z \in \mathbb{R}^d : \rho_A(z, U_j; 0) \leq \eta\}$$

where $\eta > 0$ is fixed and small enough. Let $M_j = \mathbb{R}^d \setminus [\cup_{\ell \neq j} B_{\ell,\eta}]$ and let \mathcal{P}_j be the Dirichlet realization \mathcal{H} on M_j .

Remark 3.1. In fact, we may also introduce the single well Schrödinger operator formally defined by $\mathcal{H}_j = -\frac{\hbar^2}{2m}\Delta + \mathcal{V}_j$ on $L^2(\mathbb{R}^d)$ where $\mathcal{V}_j = \phi_j \mathcal{V}$; ϕ_j is a smooth function with values in $[0, 1]$ such that

$$\phi_j(z) = \begin{cases} 0 & \text{if } z \notin B_{j,2\eta} \\ 1 & \text{if } z \in B_{j,\eta} \end{cases}.$$

That is \mathcal{V}_j is, in fact, the single well potential obtained by filling all the wells, but the j th one. Then, in the semiclassical limit, the discrete spectrum of \mathcal{P}_j coincides with the one of \mathcal{H}_j , $j = 1, \dots, N$.

Let $I(\hbar) = [\tilde{\alpha}(\hbar), \tilde{\beta}(\hbar)]$ be a given interval such that

$$\lim_{\hbar \rightarrow 0} \tilde{\alpha}(\hbar) = \lim_{\hbar \rightarrow 0} \tilde{\beta}(\hbar) = 0.$$

By construction, the spectrum of $\sigma(\mathcal{H})$ of \mathcal{H} in the interval $I(\hbar)$ is purely discrete, as well as the spectrum $\sigma(\mathcal{P}_j)$ of each \mathcal{P}_j . Then (see Theorem 4.2.1 [27]) it is possible to prove that there exists a one-to-one correspondence

$$b : \cup_{j=1}^N [\sigma(\mathcal{P}_j) \cap I(\hbar)] \rightarrow \sigma(\mathcal{H}) \cap I(\hbar)$$

such that

$$|b(\lambda) - \lambda| \leq C e^{-c/\hbar}, \quad \forall \lambda \in \sigma(\mathcal{P}_j) \cap I(\hbar),$$

for some $C > 0$ and $c > 0$ independent of \hbar and λ .

Let n (resp. n_j) be the cardinality of the set of discrete eigenvalues (counting multiplicity) of \mathcal{H} (resp. \mathcal{H}_j) in $I(\hbar)$, by the above result it follows that $n = \sum_{j=1}^N n_j$; and let us denote by ψ_m the normalized wavefunction associated to $\mathcal{E}_m \in \sigma(\mathcal{H}) \cap I(\hbar)$, $m = 1, \dots, n$, and by $\varphi_{j,\ell}$ those associated to $\mu_{j,\ell} \in \sigma(\mathcal{P}_j) \cap I(\hbar)$, $\ell = 1, \dots, n_j$. Let χ_j be the smooth function with values in $[0, 1]$ which is zero in the neighbourhoods $B_{\ell,\eta}$ of the wells U_ℓ and one outside the larger neighbourhoods $B_{\ell,2\eta}$ containing the wells U_ℓ , for $\ell \neq j$; let

$$\Psi_{j,k} = \chi_j \varphi_{j,k}, \quad k = 1, 2, \dots, n_j.$$

If we denote by Π_F the eigenprojector operator associated to the eigenspace F of \mathcal{H} in $I(\hbar)$ then we set

$$v_{j,k} = \Pi_F \Psi_{j,k};$$

this family of vectors can be proved to be a basis of the space F and we denote by $e_{j,k}$ its orthonormal realization. By construction the vectors $\varphi_{j,k}$, $\Psi_{j,k}$, $v_{j,k}$ and $e_{j,k}$ are essentially supported on the set $B_{j,\eta}$ containing the well U_j ; in particular

$$\int_{B_{j,\eta}} |e_{j,k}|^2 dz \sim 1 \quad \text{and} \quad \int_{\mathbb{R}^d \setminus B_{j,\eta}} |e_{j,k}|^2 dz \sim 0 \quad \text{as } \hbar \ll 1, \quad \text{for any } k = 1, \dots, n_j.$$

3.3.2. Application to the stable double-well model

We restrict now our analysis to the one-dimensional (i.e. $d = 1$) double-well case (i.e. $N = 2$), where we choose the interval $I(\hbar)$ such that it contains just two discrete and simple eigenvalues $\sigma(\mathcal{P}_j) \cap I(\hbar) = \{\mu_j\}$, $j = 1, 2$; in such a case $n_1 = n_2 = 1$ and thus we simply denote μ_j for $\mu_{j,1}$, e_j for $e_{j,1}$, and so on. Then (see Theorem 4.3.4 and formula (4.3.29) by [27]) in the semiclassical limit $\hbar \ll 1$ it follows that the restriction of \mathcal{H} to the eigenspace F is simply described by means of the 2×2 matrix:

$$\begin{pmatrix} \mu_1 & \beta \\ \beta & \mu_2 \end{pmatrix} + O(\hbar^\infty) e^{-\rho_i/\hbar} \quad \text{as } \hbar \ll 1 \tag{19}$$

where β is a real-valued coupling parameter such that $\beta = O(\hbar^{-N_0}) e^{-\rho_i/\hbar}$ for some $N_0 \in \mathbb{N}$ and where $\rho_i := \rho_A(U_1, U_2; 0) > 0$ is the Agmon distance between the two wells U_1 and U_2 .

Therefore $\sigma(\mathcal{H}) \cap I(\hbar)$ has only two eigenvalues $\mathcal{E}_{1,2}$ approximated by the two eigenvalues of the matrix in (19):

$$\mathcal{E}_j = \frac{1}{2}(\mu_1 + \mu_2) + (-1)^j \frac{1}{2} \sqrt{(\mu_1 - \mu_2)^2 + 4\beta^2} + O(\hbar^\infty) e^{-\rho_i/\hbar}, \quad j = 1, 2,$$

with associated normalized wavefunctions

$$\psi_j \sim u_{1,j} e_1 + u_{2,j} e_2, \quad \text{as } \hbar \ll 1;$$

where $u_j = \begin{pmatrix} u_{1,j} \\ u_{2,j} \end{pmatrix} = \frac{w_j}{|w_j|}$ are the normalized eigenvectors of the matrix; that is:

$$w_j = \begin{pmatrix} 1 \\ \frac{\mu_1 - \mathcal{E}_j}{\beta} \end{pmatrix} = \begin{pmatrix} 1 \\ \frac{1}{2\beta}(\mu_1 - \mu_2) - (-1)^j \frac{1}{2\beta} \sqrt{(\mu_1 - \mu_2)^2 + 4\beta^2} \end{pmatrix}. \tag{20}$$

In conclusion; when we are in a neighbourhood of the crossing point, that is $|\mu_1 - \mu_2| \ll |\beta|$, then

$$w_j \sim \begin{pmatrix} 1 \\ -(-1)^j \end{pmatrix} \Rightarrow u_j \sim \begin{pmatrix} 1/\sqrt{2} \\ -(-1)^j/\sqrt{2} \end{pmatrix}, \text{ as } \hbar \ll 1,$$

which means that the two wavefunctions are both equally supported within the two wells. On the other hands, if we are far from the crossing point, that is when $|\mu_1 - \mu_2| \gg |\beta|$, then

$$w_1 \sim \begin{pmatrix} 1 \\ \frac{\mu_1 - \mu_2}{\beta} \end{pmatrix} \text{ and } w_2 \sim \begin{pmatrix} 1 \\ 0 \end{pmatrix}, \text{ as } \hbar \ll 1,$$

that is

$$u_1 \sim \begin{pmatrix} 0 \\ 1 \end{pmatrix} \text{ and } u_2 \sim \begin{pmatrix} 1 \\ 0 \end{pmatrix}, \text{ as } \hbar \ll 1,$$

which means that one wavefunction is supported within one well and the other wavefunction is supported within the other well.

We can summarize these semiclassical arguments in the following proposition:

Proposition 3.1. *In a stable double-well model the (avoided) crossing of isolated doublets of eigenvalues $E_{1,2}$ is related to the fact that the associated wavefunctions $\psi_{1,2}$ are equally supported within both wells in the sense that $P_{j,\ell} \sim P_{j,r} \sim \frac{1}{2}$, $j = 1, 2$, as \hbar goes to zero, in a neighbourhood of the crossing point. On the contrary, when we are far from the crossing point then each associated wavefunction is supported within just one well.*

Remark 3.2. This theoretical result, which holds true in the semiclassical limit as \hbar goes to zero, is in a good agreement with the numerical experiments (see Figs. 4 and 5) obtained for a fixed value of the Planck constant. In fact, potential $\mathcal{V}_{v_1, v_2, v_3}$ does not satisfies the above regularity assumptions; however, we could regularize it in order to fit with the conditions of [27].

4. Unstable double-well model

Here we consider the spectral properties of the Schrödinger operator H formally defined by (12) where, in dimensionless units, the *unstable* potential $V_{\alpha_1, \alpha_2, \alpha_3}(x)$ is the piecewise constant function (9) with $\alpha_3 \leq \min(\alpha_1, \alpha_2) < 0$ (see Fig. 1 - broken line). Thus, the two (internal) wells correspond to the intervals (x_1, x_2) and (x_3, x_4) , and the two barriers correspond to the interval (x_2, x_3) , conventionally denoted *internal* (or *inner*) barrier, and to the interval (x_4, x_5) , conventionally denoted *external* (or *outer*) barrier.

In contrast to the case discussed in Section 3, where for $\alpha_3 = 0$ the operator H may have eigenvalues, in the case $\alpha_3 \leq \min\{\alpha_1, \alpha_2\}$ it cannot have eigenvalues, but quantum resonances associated to metastable states, and for such a reason we call $V_{\alpha_1, \alpha_2, \alpha_3}$ an *unstable* double-well potential. In fact, quantum resonances have a strictly negative imaginary part, and the discussion of their intersection as the model's parameters vary is much more intricate than the one discussed in Section 3 in the case of real-valued eigenvalues. More precisely, we recall that we may have two types of crossings between two resonances E_1 and E_2 :

- Type *I* crossing when there is an exact crossing of the imaginary part of the resonances, i.e. $\Im E_1 = \Im E_2$, and an avoided crossing of their real parts;
- Type *II* crossing when there is an exact crossing of the real part of the resonances, i.e. $\Re E_1 = \Re E_2$, and an avoided crossing of their imaginary parts.

With more details, it is well known that $\sigma(H) = \sigma_{ess}(H) = [\alpha_3, +\infty)$ if $\alpha_3 \leq \alpha_{1,2}$, and then the discrete spectrum is empty and there are no eigenvalues. Eventually, there exists quantum resonances defined by means of the matching conditions

$$\psi(x) \text{ and } \frac{d\psi(x)}{dx} \text{ continuous at } x_n, \quad n = 1, \dots, 5, \tag{21}$$

and from the outgoing conditions

$$\psi(x) \rightarrow 0 \text{ as } x \rightarrow -\infty$$

and (Siegert's approximation method, see i.e. [8])

$$\psi(x) = e^{ih_3x} \text{ for } x > x_5, \text{ where } h_3 = \sqrt{E - \alpha_3}.$$

Because E can take complex values, it is necessary to specify how the cut in the complex plane for the square root function is chosen; we define \sqrt{w} for $w \in \mathbb{C} \setminus [0, +\infty)$ such that $\Im \sqrt{w} > 0$, everywhere; for $w \in [0, +\infty)$ we write $\sqrt{w} = \sqrt{w} + i0$.

The general solution to equation $H\psi = E\psi$ satisfying the outgoing conditions, where $\Re E \in (\alpha_3, 0)$ and $\Im E < 0$, is

$$\psi(x) = \begin{cases} a \exp(kx) & \text{if } x < x_1 \quad := 0 \\ b \cos(h_1x) + c \sin(h_1x) & \text{if } x_1 < x < x_2 \\ d \exp(kx) + e \exp(-kx) & \text{if } x_2 < x < x_3 \\ f \cos(h_2x) + g \sin(h_2x) & \text{if } x_3 < x < x_4 \\ h \exp(kx) + \ell \exp(-kx) & \text{if } x_4 < x < x_5 \\ m \exp(ih_3x) & \text{if } x_5 < x \end{cases}$$

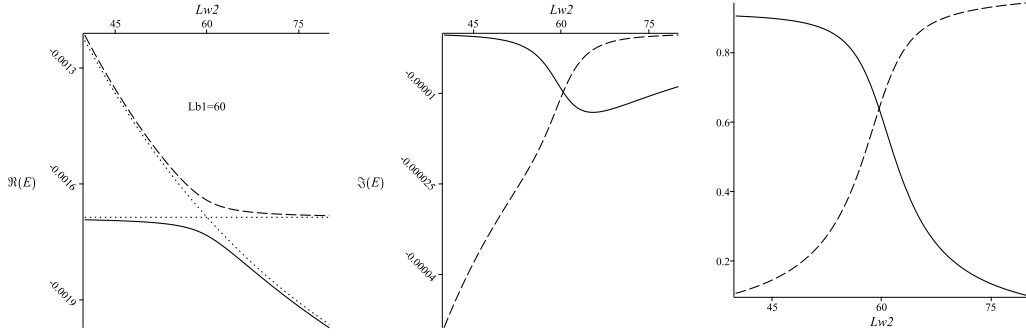


Fig. 5. Let $L_{b_1} = 60$. Here we plot the real part (left hand side panel) and the imaginary part (central panel) of the two resonances E_1 (full line) and E_2 (broken line); dot lines correspond the real part of the quantum resonances of the two unstable single well operators. In this case we observe a type *I* crossing. In the right hand side panel we plot the quantities $P_{1,l}$ (full line) and $P_{1,r}$ (broken line).

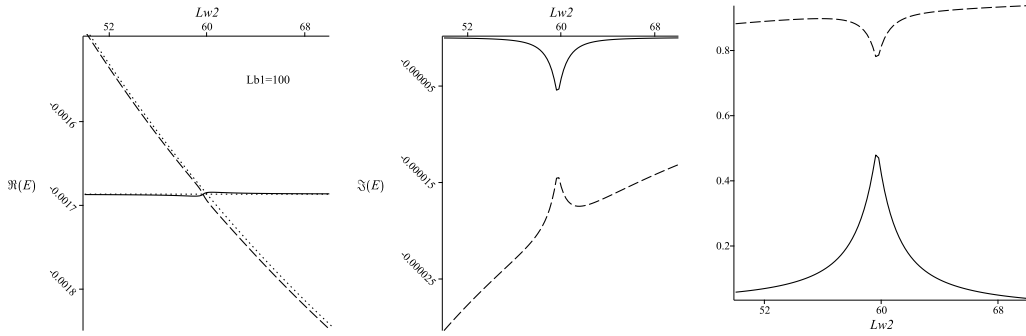


Fig. 6. Let $L_{b_1} = 100$. Here we plot the real part (left hand side panel) and the imaginary part (central panel) of the two resonances E_1 (full line) and E_2 (broken line); dot lines correspond the real part of the quantum resonances of the two unstable single well operators. In this case we observe a type *II* crossing. In the right hand side panel we plot the quantities $P_{1,l}$ (full line) and $P_{1,r}$ (broken line).

where

$$k = \sqrt{-E} \quad \text{and} \quad h_j = \sqrt{E - \alpha_j}, \quad j = 1, 2, 3.$$

Here, for the sake of simplicity, in the numerical experiments we assume that the unstable double-well is such that

$$\alpha := \alpha_1 = \alpha_2 = \alpha_3 < 0.$$

4.1. Resonances crossing in an unstable double-well model

We consider two numerical experiments, one with a (relatively) small internal barrier, and the other one with a (relatively) large external barrier. In both models:

- The heterostructure parameter s is chosen such that $\alpha := \alpha_{1,2,3} = -0.264(4) \cdot 10^{-2}$ in dimensionless units.
- The left hand side well has length $L_{w_1} = 60$ in dimensionless units.
- The external barrier has length $L_{b_2} = 40$ in dimensionless units.
- In the first experiment the internal barrier has length $L_{b_1} = 60$ in dimensionless units; in the second experiment the length of the internal barrier is larger, i.e. $L_{b_1} = 100$ in dimensionless units.
- The value, in dimensionless units, of the length L_{w_2} of the right hand side well runs between 40 and 80.

Let E_1 and E_2 be the two resonances of H with lower energy levels; when L_{w_2} runs in the interval $[40, 80]$ the real and imaginary parts of these two resonances vary and, for a critical value for L_{w_2} , they may cross. From the numerical experiments it turns out that when the length of the internal barrier is small enough, e.g. $L_{b_1} = 60$ in dimensionless units, then the crossing point is for L_{w_2} close to the value of L_{w_1} and one can observe in Fig. 5 a type *I* crossing. On the other side, when the length of the internal barrier is large enough, e.g. $L_{b_1} = 100$ in dimensionless units, then also in this case the crossing point is for L_{w_2} close to the same value as before but, as one can observe in Fig. 6, a type *II* crossing occurs.

As done in Section 3, even in the case of resonances we can estimate how much each metastable state ψ_j associated to the resonance E_j , $j = 1, 2$, is supported within one of the two wells by means of the quantities $P_{j,\ell}$ defined in (17).

Remark 4.1. We have to stress that the normalization condition for metastable states must be discussed; in our numerical experiments, for argument's sake, we assume the normalization condition on the two wells; that is we assume that

$$\int_{x_1}^{x_4} |\psi_j(x)|^2 dx = 1, \quad j = 1, 2.$$

In Fig. 5 - right hand side panel - we plot the functions $P_{1,\ell}$ and $P_{1,r}$ for $L_{b_1} = 60$ and we see that at the crossing point of the imaginary parts of the two resonances there is an interchange of the well where ψ_1 is mostly supported; a similar result holds true for ψ_2 . In contrast, in Fig. 6 - right hand side panel - we plot the functions $P_{1,\ell}$ and $P_{1,r}$ for $L_{b_1} = 100$ and we see that in this case there is no an interchange of the well where ψ_1 is mostly supported; a similar result holds true for ψ_2 . Thus, we can conjecture that *in an unstable double-well model the crossing phenomenon of type I of quantum resonances is associated with the interchange of the well where each metastable state is mostly supported; on the other hand, in the case of crossing phenomenon of type II of quantum resonances there is no interchange of the well where each metastable state is mostly supported.*

4.2. Explanation of the resonances crossing in the semiclassical limit

Even in the case of quantum resonances a result similar to the one given in Section 3.3 holds true for the operator

$$\mathcal{H} = -\frac{\hbar^2}{2m} \frac{d^2}{dz^2} + \mathcal{V}, \tag{22}$$

where \mathcal{V} is an unstable double-well potential with two minimum points z_1 and z_2 such that

$$\mathcal{V}_{min} := \mathcal{V}(z_1) = \mathcal{V}(z_2) \geq \mathcal{V}_\infty := \liminf_{|z| \rightarrow \infty} \mathcal{V}(z).$$

Also in this section, for argument's sake, we fix the units such that $2m = 1$.

In fact, in the semiclassical limit $\hbar \ll 1$ and under the assumption that the unstable double-well potential \mathcal{V} is an analytic function satisfying some technical assumptions (see Hypotheses 1–3 in [4,5]) has been proved that the reduction to a 2×2 matrix of the form (19) gives the two resonances and the associated metastable states; furthermore, a criterion in order to establish the kind of crossing has been provided. These results can be summarized as follows.

For some fixed $\mathcal{E} > \mathcal{V}_{min}$ then $\mathcal{V}^{-1}((-\infty, \mathcal{E}]) = U_1 \cup U_2 \cup O$, where the two wells U_1 and U_2 are compact and disjoint sets with zero diameter with respect to the Agmon distance, and where O is an unbounded set. For instance, if \mathcal{V} is the square potential $\mathcal{V}_{v_1, v_2, v_3}$ as in Fig. 1 – broken line – and $\max\{v_1, v_2, v_3\} < \mathcal{E} < 0$ then $U_1 = [z_1, z_2]$ and $U_2 = [z_3, z_4]$ are the two wells, $[z_2, z_3]$ is the *internal* (or *inner*) barrier, $[z_4, z_5]$ is the *external* (or *outer*) barrier and $O = [z_5, +\infty)$.

Let $\mathcal{H}_j = -\hbar^2 \frac{d^2}{dz^2} + \mathcal{V}_j$, $j = 1, 2$, be the two single well Schrödinger operators defined as in Remark 3.1 ; then, one can prove that (see [4] and, in particular, Lemma 13) \mathcal{H}_j has a ground state resonance μ_j such that $\Re \mu_j \sim \mu_j^D$, where μ_j^D is the discrete ground state eigenvalue of the operator \mathcal{P}_j defined in Section 3.3 with zero Dirichlet boundary condition outside a neighbourhood of the j th well U_j . Furthermore,

$$\Im(\mu_j) = -\tilde{\phi}_j e^{-2\rho_A(U_j, O; \mu_j^D)/\hbar}, \quad j = 1, 2,$$

where

$$\rho_A(U_j, O; \mu_j^D) := \inf_{z \in \partial U_j, \zeta \in \partial O} \rho_A(z, \zeta; \mu_j^D)$$

is the Agmon's distance between the well U_j and O and where $\tilde{\phi}_j$, $j = 1, 2$, are positive constants such that

$$C^{-1} \hbar^{-1/2} \leq \tilde{\phi}_j \leq C \hbar^{1/2} \tag{23}$$

for some positive constant C . In order to study the crossing scenario we observe that, by varying the values of the parameters of the model, we may have that $\Re \mu_1$ and $\Re \mu_2$ take the same value μ ; this is the crossing point. Assume that at this crossing point we have that $\rho_A(U_1, O; \mu) = \rho_i + \rho_e$ where $\rho_i := \rho_A(U_1, U_2; \mu)$ is the Agmon's length of the internal barrier and $\rho_e := \rho_A(U_2, O; \mu)$ is the Agmon's length of the external barrier. For instance, in the case where $\mathcal{V} = \mathcal{V}_{v_1, v_2, v_3}$ then this condition is fulfilled where

$$\rho_i = \rho_A(z_2, z_3; \mu) \quad \text{and} \quad \rho_e = \rho_A(z_4, z_5; \mu).$$

Then, similarly to Section 3.3, we can compute the resonances of $\mathcal{H} = -\hbar^2 \frac{d^2}{dz^2} + \mathcal{V}$ by means of the reduction to the 2×2 matrix (19), with a different remainder term (see [4,5] for details), where the *complex-valued* coupling term β is such that $\beta \sim \tilde{\phi} e^{-\rho_i/\hbar}$ as \hbar goes to zero, and where $|\tilde{\phi}|$ satisfies (23). Therefore, the two ground state resonances of \mathcal{H} are given by

$$E_{1,2} \sim \frac{1}{2}(\mu_1 + \mu_2) \pm \sqrt{\frac{1}{4}(\mu_1 - \mu_2)^2 + \beta^2}, \quad \text{as } \hbar \ll 1.$$

From this fact it follows that in the semiclassical limit $\hbar \ll 1$ and in a neighbourhood of the crossing point the unstable double-well operator \mathcal{H} has two resonances $\mathcal{E}_{1,2}$ with real part close to μ . In particular, we have that

$$\mathcal{E}_{1,2} \sim \mu - i \frac{1}{2} \tilde{\phi}_2 e^{-2\rho_e/\hbar} \pm \frac{1}{2} \sqrt{-\tilde{\phi}_2^2 e^{-4\rho_e/\hbar} + \tilde{\phi}^2 e^{-2\rho_i/\hbar}}, \text{ as } \hbar \ll 1,$$

at the crossing point where $\mu := \Re \mu_1 = \Re \mu_2$. Therefore

- if $\rho_i < 2\rho_e$ then

$$\mathcal{E}_{1,2} \sim \mu - i \frac{1}{2} \tilde{\phi}_2 e^{-2\rho_e/\hbar} \pm \frac{1}{2} \tilde{\phi} e^{-\rho_i/\hbar}, \text{ as } \hbar \ll 1,$$

and so we observe a type *I* crossing;

- if $\rho_i > 2\rho_e$ then

$$\mathcal{E}_{1,2} \sim \mu - i \frac{1}{2} \tilde{\phi}_2 e^{-2\rho_e/\hbar} \pm i \frac{1}{2} \tilde{\phi}_2 e^{-2\rho_e/\hbar}, \text{ as } \hbar \ll 1,$$

and so we observe a type *II* crossing.

For what concerns the metastable states $\psi_{1,2}$ associated with $\mathcal{E}_{1,2}$ it turns out that the two eigenvectors w_j of the 2×2 matrix are given by (20). Therefore, at the crossing point where $\Re \mu_1 = \Re \mu_2$ then

$$w_j \sim \begin{pmatrix} 1 \\ \frac{-\tilde{\phi}_2 e^{-2\rho_e/\hbar}}{2\tilde{\phi} e^{-\rho_i/\hbar}} - (-1)^j \sqrt{\frac{\tilde{\phi}_2^2 e^{-2(2\rho_e - \rho_i)/\hbar}}{4\tilde{\phi}^2} + 1} \end{pmatrix} \text{ as } \hbar \ll 1.$$

Hence,

- if $\rho_i < 2\rho_e$ then

$$w_j \sim \begin{pmatrix} 1 \\ -(-1)^j \end{pmatrix}, \tag{24}$$

the normalized eigenvectors u_j of the 2×2 matrix are given by

$$u_j \sim \begin{pmatrix} 1/\sqrt{2} \\ -(-1)^j/\sqrt{2} \end{pmatrix} \tag{25}$$

and the metastable states $\psi_{1,2}$ are equally supported within both wells.

- if $\rho_i > 2\rho_e$ then

$$w_1 \sim \begin{pmatrix} 1 \\ 0 \end{pmatrix} \text{ and } w_2 \sim \begin{pmatrix} 1 \\ \frac{\tilde{\phi}_2}{\tilde{\phi}} e^{-(2\rho_e - \rho_i)/\hbar} \end{pmatrix}, \tag{26}$$

the normalized eigenvectors u_j of the 2×2 matrix are given by

$$u_1 \sim \begin{pmatrix} 1 \\ 0 \end{pmatrix} \text{ and } u_2 \sim \begin{pmatrix} 0 \\ 1 \end{pmatrix} \tag{27}$$

and the metastable states $\psi_{1,2}$ are mostly supported within different wells.

We can summarize these semiclassical arguments in the following proposition:

Proposition 4.1. *In an unstable double-well model the crossing of the two resonances $\mathcal{E}_{1,2}$ can generically be of type *I* or *II*. In particular, in the semiclassical limit $\hbar \ll 1$:*

- if $\rho_i < 2\rho_e$ then we have a type *I* crossing;
- if $\rho_i > 2\rho_e$ then we have a type *II* crossing;

where ρ_i is the Agmon length of the internal barrier and ρ_e is the Agmon length of the external one.

Furthermore, in the case of type *I* crossing the associated metastable states $\psi_{1,2}$ are equally supported within both wells in the sense that $P_{j,\ell} \sim P_{j,r} \sim \frac{1}{2}$, $j = 1, 2$, as \hbar goes to zero, in a neighbourhood of the crossing point. On the contrary, when we are far from the crossing point or when we are in the case of type *II* crossing then the two metastable states are mostly supported within different wells.

Remark 4.2. In the one dimensional model (22) where the potential \mathcal{V} is given by the piecewise constant function (9) we have that

$$\rho_i := \int_{z_2}^{z_3} \sqrt{\mathcal{V}_{v_1, v_2, v_3}(z) - \mu} dz = (z_3 - z_2) \sqrt{-\mu} = \ell_{b_1} \sqrt{-\mu}$$

and

$$\rho_e := \int_{z_4}^{z_5} \sqrt{\mathcal{V}_{v_1, v_2, v_3}(z) - \mu} dz = (z_5 - z_4) \sqrt{-\mu} = \ell_{b_2} \sqrt{-\mu}.$$

Therefore, in the first experiment where $\ell_{b_1} = 60 \text{ \AA}$ and $\ell_{b_2} = 40 \text{ \AA}$ then

$$\frac{\rho_i}{2\rho_e} = \frac{\ell_{b_1}}{2\ell_{b_2}} = \frac{3}{4} < 1,$$

and there is a good agreement between the semiclassical result and the kind of crossing (see Fig. 5). In the second experiment where $\ell_{b_1} = 100 \text{ \AA}$ and $\ell_{b_2} = 40 \text{ \AA}$ then

$$\frac{\rho_i}{2\rho_e} = \frac{\ell_{b_1}}{2\ell_{b_2}} = \frac{5}{4} > 1.$$

and also in this case there is a good agreement between the semiclassical result and the kind of crossing (see Fig. 6). As discussed in Remark 3.2 we could think to regularize the potential $\mathcal{V}_{v_1, v_2, v_3}$ in order to fit wit Hypotheses 1–3 [4,5] ; however, we do not dwell here on such a technical problem.

5. Survival amplitude

It is important to note that the time behaviour of some physical observables depends on the type of crossing of the resonances. Let us consider, for example, the survival amplitude $\mathcal{A}(t) = \langle \psi_0 | \psi \rangle$ where ψ_0 is the wave function of the initial state at t_0 (for sake of simplicity we may always assume that $t_0 = 0$), and where $\psi = e^{-iHt} \psi_0$ is the wavefunction of the state at instant t ; i.e. it satisfies to the time dependent Schrödinger equation in dimensionless units (14). In the double-well model considered in the previous section where we have two resonances E_1 and E_2 then the behaviour of the survival amplitude is expected to be given, at intermediate times, by formula (4).

If the model's parameters are such that we are in the case of type *II* crossing or if we are in the case of type *I* crossing but we are far enough from the crossing point then $\Im E_1 \neq \Im E_2$ and thus one of the two terms e^{-itE_j} decays much faster than the other one. Hence, we expect to observe an exponentially decreasing behaviour of $\mathcal{A}(t)$ without significant oscillations.

On the other side, if we are in the case of type *I* crossing and the model's parameters are such that $\Im E_1 = \Im E_2$, then there is a damped oscillating behaviour due to the interference effect between the two resonances, and in this case the dominant behaviour of $|\mathcal{A}(t)|$ is given by:

$$e^{-t|\Im E_1|} |c_{E_1} + c_{E_2} e^{-i\omega t}|, \tag{28}$$

with pseudo-period $T = 2\pi/\omega$ where $\omega = \Re E_2 - \Re E_1$.

Therefore, we can conjecture that *when we have a resonances crossing of type I and $\Im E_1$ is quite close to $\Im E_2$ then we expect to observe a damped oscillating behaviour for the survival amplitude $\mathcal{A}(t)$. On the other hand, when we have a resonances crossing of type II or in the case of type I, with the model's parameters such that $\Im E_1$ is quite different from $\Im E_2$, then we expect to observe a damped behaviour of the survival amplitude without significative oscillations.*

This scenario becomes more evident when one chooses the initial state ψ_0 prepared within only one of the two wells. In fact, in such a case if $\Im E_1$ is different enough from $\Im E_2$ then one of the two coefficients c_{E_1} and c_{E_2} is negligible because one of the wave functions $\psi_{1,2}$ of the metastable states is supported within one well and the other one is supported within the other well; hence, from (3) one of the coefficients c_{E_j} is expected to be very small (in absolute value).

We compute now the survival amplitude for the unstable double-well model introduced in Section 4 by making use of formula (4) and also by making use of the spectral splitting method in order to numerically test the validity of (4) in an explicit model.

5.1. Survival amplitude in the unstable double-well model

We consider two numerical experiments for the Hamiltonian (12), one with a (relatively) small internal barrier such that we have a resonances crossing of type *I*, and the other one with a (relatively) large external barrier such that we have a resonances crossing of type *II*. In both models:

- The heterostructure is chosen such that $\alpha := \alpha_{1,2,3} = -0.264(4) \cdot 10^{-2}$ in dimensionless units.
- The left hand side well has length $L_{w_1} = 60$ in dimensionless units.
- The external barrier has length $L_{b_2} = 40$ in dimensionless units.

We assume, for argument's sake, that the initial normalized wavefunction ψ_0 coincides with the ground state normalized wavefunction of the single well operator formally defined by $H_1 = -\frac{d^2}{dx^2} + V_{\alpha_1, 0, 0}$ on $L^2(\mathbb{R}, dx)$. For $L_{w_1} = 60$ and $\alpha_1 = -0.264(4) \cdot 10^{-2}$ then H_1 has a ground state with energy

$$E_0 = -0.168(7) \cdot 10^{-2}$$

and

$$\psi_0(x) = C \begin{cases} e^{kx} & \text{if } x \leq x_1 := 0 \\ \cos(hx) + 1.330(3) \sin(hx) & \text{if } x_1 < x < x_2 := x_1 + L_{w_1} \\ 11.757(2)e^{-kx} & \text{if } x_2 \leq x \end{cases}, \tag{29}$$

Table 1

Table of values of the resonances E_j and of the coefficients c_{E_j} , $j = 1, 2$, for different values of L_{w_2} ; where $L_{b_1} = 60$ corresponds to a type I crossing. The exact crossing of the imaginary part occurs at $L_{w_2} = 60.341(2)$. Calculation of ω and T makes sense only when $\Im E_1 \approx \Im E_2$, that is for L_{w_2} close to 60.

	$L_{w_2} = 50$	$L_{w_2} = 60$	$L_{w_2} = 70$
$\Re E_1$	$-0.169(9) \cdot 10^{-2}$	$-0.173(4) \cdot 10^{-2}$	$-0.185(6) \cdot 10^{-2}$
$\Im E_1$	$-0.119(1) \cdot 10^{-5}$	$-0.931(7) \cdot 10^{-5}$	$-0.122(1) \cdot 10^{-4}$
$\Re E_2$	$-0.147(5) \cdot 10^{-2}$	$-0.164(3) \cdot 10^{-2}$	$-0.167(7) \cdot 10^{-2}$
$\Im E_2$	$-0.296(0) \cdot 10^{-4}$	$-0.106(2) \cdot 10^{-4}$	$-0.117(3) \cdot 10^{-5}$
ω		$0.910(2) \cdot 10^{-4}$	
T		$0.690(3) \cdot 10^5$	
$\Re c_{E_1}$	0.933(4)	0.427(4)	$0.527(3) \cdot 10^{-1}$
$\Im c_{E_1}$	$0.382(9) \cdot 10^{-2}$	$0.134(9) \cdot 10^{-1}$	$0.215(3) \cdot 10^{-2}$
$\Re c_{E_2}$	$0.293(1) \cdot 10^{-1}$	0.415(8)	0.915(6)
$\Im c_{E_2}$	$0.302(7) \cdot 10^{-2}$	$0.150(0) \cdot 10^{-1}$	$0.361(4) \cdot 10^{-2}$

where

$$k = \sqrt{-E_0} = 0.0410(7) \quad \text{and} \quad h = \sqrt{E_0 - \alpha_1} = 0.0308(3)$$

and

$$C = 0.0815(1)$$

is a normalization factor.

5.1.1. Type I crossing - $L_{b_1} = 60$

In this case the internal barrier has length $L_{b_1} = 60$ in dimensionless units; then, see Section 4.1, we have a resonances crossing of type I . We consider then the cases where the right hand side well has length

- i. $L_{w_2} = 50$ in dimensionless units;
- ii. $L_{w_2} = 60$ in dimensionless units;
- iii. $L_{w_2} = 70$ in dimensionless units.

In Table 1 are collected the values of E_j , $j = 1, 2$. It turns out that in the cases $L_{w_2} = 50$ and $L_{w_2} = 70$ the term $\Im E_1$ is quite different from $\Im E_2$ and thus from (4) we expect to observe an exponentially damping behaviour of $\mathcal{A}(t)$ without significant oscillations because the interference effect between the two metastable states is not triggered for two reasons:

- one metastable state decays much more faster than the second one;
- one metastable state is mostly supported within one well while the other metastable state is mostly supported within the other one (see Fig. 5), hence we have that $|c_{E_1}| \approx 1$ while $|c_{E_2}| \approx 0$ (or vice versa).

On the other hand, in the case ii. where $L_{w_2} = 60$ we expect to observe oscillations of $\mathcal{A}(t)$ because $\Im E_1 \approx \Im E_2$ (in fact, the exact crossing point for the imaginary part of resonances is for $L_{w_2} = 60.341(2)$) and then an interference effect is triggered; furthermore, in such a case the two metastable states are equally supported within both wells (see Fig. 5 again) and then we have that $|c_{E_1}| \approx |c_{E_2}|$.

Remark 5.1. This result qualitatively agrees with the numerical calculation of $|\mathcal{A}(t)|$ (see Fig. 7 - right hand side panel) obtained by making use of the spectral splitting method (see Appendix). In fact, in correspondence of a resonances crossing for $L_{w_2} = 60$ in both pictures an oscillating beating behaviour (full line in Fig. 7) occurs where the (pseudo-)period obtained in Table 1 by means of the imaginary part of the resonances practically coincides with the one of the figure constructed by means of the spectral splitting approximation. The calculation based on the spectral splitting approximation was carried out by means of a Fortran programme running on an iMac Chip Apple M1 - 8 core processor with 8 GB of RAM for 62 h and 17 min; the spatial mesh consists of the division of the interval $[-140, 360]$ into 20000 points, 10000 time iterations were carried out for t varying in the interval $[0, 50000]$.

5.1.2. Type II crossing

In this case the internal barrier has length $L_{b_1} = 100$ in dimensionless units and, see Section 4, we have a resonances crossing of type II and thus $\Im E_1$ is quite different from $\Im E_2$ for any value of L_{w_2} . In particular, we consider then the cases where the right hand side well has length

- i. $L_{w_2} = 50$ in dimensionless units;
- ii. $L_{w_2} = 60$ in dimensionless units;
- iii. $L_{w_2} = 70$ in dimensionless units.

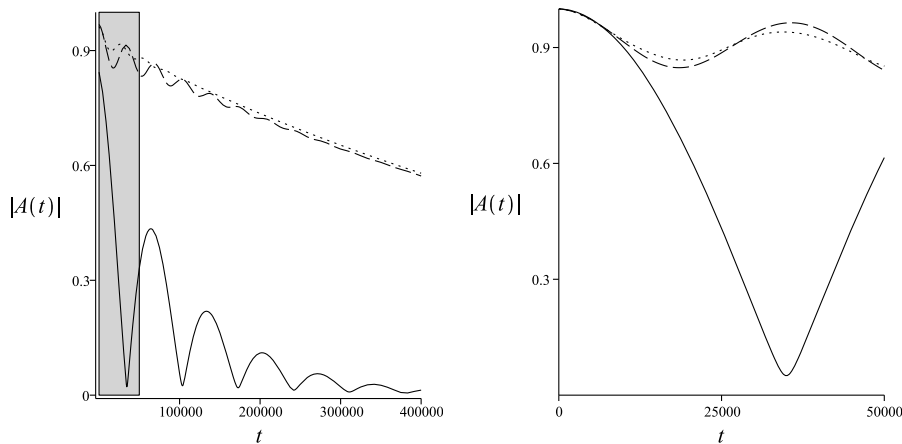


Fig. 7. Beating behaviour of $|A(t)|$, $t \in [0, 4 \cdot 10^5]$, in the case of type *I* crossing for $L_{b_1} = 60$. Dot line corresponds to the case $L_{w_2} = 50$, broken line corresponds to the case $L_{w_2} = 70$. Significant oscillations are observed (full line) only when we are close to the crossing point, that is for $L_{w_2} = 60$; we recall that we have an exact crossing of the imaginary part of the two resonances when $L_{w_2} = 60.341(2)$. In the left hand side panel $A(t)$ is computed by means of formula (4). In the right hand side panel $A(t)$ is computed for $t \in [0, 5 \cdot 10^4]$ (which corresponds to the box in the left hand side picture) by means of the spectral splitting method; a good qualitative agreement, that is significant oscillations only occur for L_{w_2} close to the crossing point, between the two calculation methods emerges.

Table 2

Table of values of the resonances E_j and of the coefficients c_{E_j} , $j = 1, 2$, for different values of L_{w_2} ; where $L_{b_1} = 100$ corresponds to a type *II* crossing. Since $\Im E_1$ is quite different from $\Im E_2$ then the calculation of ω and T does not make sense.

	$L_{w_2} = 50$	$L_{w_2} = 60$	$L_{w_2} = 70$
$\Re E_1$	$-0.168(7) \cdot 10^{-2}$	$-0.169(5) \cdot 10^{-2}$	$-0.184(8) \cdot 10^{-2}$
$\Im E_1$	$-0.554(8) \cdot 10^{-7}$	$-0.154(6) \cdot 10^{-4}$	$-0.131(7) \cdot 10^{-4}$
$\Re E_2$	$-0.149(1) \cdot 10^{-2}$	$-0.168(5) \cdot 10^{-2}$	$-0.168(6) \cdot 10^{-2}$
$\Im E_2$	$-0.303(5) \cdot 10^{-4}$	$-0.423(3) \cdot 10^{-5}$	$-0.495(1) \cdot 10^{-7}$
$\Re c_{E_1}$	0.996(9)	0.736(4)	0.996(4)
$\Im c_{E_1}$	$0.244(2) \cdot 10^{-3}$	$0.136(0) \cdot 10^{-1}$	$0.213(8) \cdot 10^{-3}$
$\Re c_{E_2}$	$0.138(2) \cdot 10^{-2}$	0.166(3)	$0.227(2) \cdot 10^{-2}$
$\Im c_{E_2}$	$0.190(1) \cdot 10^{-3}$	$0.112(2) \cdot 10^{-1}$	$0.128(0) \cdot 10^{-3}$

In Table 2 are collected the values of E_j , $j = 1, 2$. Since $\Im E_1$ is, in all the three cases, quite different from $\Im E_2$ then from (4) it is evident that we expect to observe an exponentially damping behaviour of $A(t)$ without significant oscillations. In fact, also in this case we checked that the numerical calculation of $A(t)$ carried out by means of the spectral splitting method fully agrees with this prediction.

6. Conclusion

The study of crossings of isolated doublets of quantum resonances opens a rich scenario for the understanding of the dynamical behaviour of some physical observables. In this work, the analysis was considered in the case of uni-dimensional double-well potentials.

Initially, a propaedeutic study restricted to the simplest case of real-valued eigenvalues is carried out; where it is shown, both numerically on a realistic model inspired by heterostructures and theoretically in the semiclassical limit, that near the (almost) crossing point of the two eigenvalues the associated eigenvectors of the quantum system tend to be equally supported within the two wells also in the case of asymmetrical double-well potential. In contrast, outside of such a neighbourhood, the eigenvectors are instead supported within just a single well.

Next, the case of quantum resonances, which have a strictly negative imaginary part, is considered, and it has been observed by numerical experiments and then demonstrated in the semiclassical limit that the effect explained above continues to exist. More precisely, in the case of resonances crossing of type *I*, where the imaginary parts of two resonances cross and where there is an avoided crossing of their real parts instead, the metastable states decay with the same speed and they are equally supported on the two wells. This fact can be associated with a damped oscillating behaviour of the survival probability because an interference phenomenon is established.

This effect underlies the proposal for a quantum sensor that can measure, quickly and easily, whether the model's parameters are closed or not to predefined values, as described in a toy model with two Dirac's δ [22], by simply observing whether the survival amplitude has a (damped) oscillating behaviour or not. This line of research deserves to be deepened with the study of a quantum sensor that checks whether an external DC electric field has a predefined value. More precisely, we can consider a heterostructure

where the electric field has the direction of the effective potential; as the electric field strength varies, the quantum resonances can cross when the strength of the DC electric field assumes a critical value, and if the nature of the crossing is of type *I*, damped oscillating behaviour of the survival probability is observed, otherwise a simple damping without beating occurs.

Declaration of competing interest

The authors declare that they have no known competing financial interests or personal relationships that could have appeared to influence the work reported in this paper.

Appendix. Spectral splitting method

The effect of the resonances, and of their associated metastable states, to the time behaviour of the survival amplitude is based on the assumption of the validity of (4) in the realistic model introduced in Section 2 inspired by heterostructures. We will check this fact by means of a numerically study of the behaviour of $\mathcal{A}(t)$ by making use of the spectral splitting approximation method we briefly resume now (see, e.g., [28,29]).

An efficient numerical treatment of the time-dependent Schrödinger equation is based on the Lie-type splitting approximation. The basic idea is quite simple: our aim is to consider an evolution equation of the type

$$\begin{cases} i \frac{\partial \psi}{\partial t} = H \psi \\ \psi|_{t=t_0} = \psi_0 \end{cases}, \psi \in L^2(\mathbb{R}, dz), \tag{30}$$

where $t_0 = 0$ and where, for argument's sake, we fix the units such that $\hbar = 1$ and $2m = 1$,

$$H = H_0 + V$$

where $H_0 = -\frac{d^2}{dx^2}$ is the free Hamiltonian and V is a real-valued potential. Let us denote by $S^t \psi_0$ the solution to (30) where $S^t = e^{-iHt}$ is the associated evolution operator; let us denote by $X^t = e^{-iH_0 t}$ and $Y^t = e^{-iVt}$ the evolution operators respectively associated to the equations

$$i \frac{\partial \psi}{\partial t} = H_0 \psi \quad \text{and} \quad i \frac{\partial \psi}{\partial t} = V \psi .$$

That is X^t is the integral operator

$$(e^{-iH_0 t} \varphi)(x) = \frac{1}{\sqrt{4\pi i t}} \int_{\mathbb{R}} e^{i(x-y)^2/4t} \varphi(y) dy$$

and $(Y^t \varphi)(x) = e^{-iV(x)t} \varphi(x)$ is a multiplication operator. It is well known that, in general,

$$S^\delta \psi_0 \neq X^\delta Y^\delta \psi_0, \quad \forall \delta \in \mathbb{R} \setminus \{0\},$$

but this difference may be proved, under some circumstances, to be small when δ is small. More precisely, if one fix any $t^* > 0$, a $\delta > 0$ small enough and a positive integer number n such that $t = n\delta < t^*$, then the solution $\psi = S^t \psi_0$ to (30) can be approximated by

$$[X^\delta Y^\delta]^n \psi_0, \tag{31}$$

up to a remainder term that goes to zero when δ goes to zero. In fact, a better result may be obtained by means of the Strang-type method where the solution ψ to (30) is approximated by

$$[X^{\delta/2} Y^\delta X^{\delta/2}]^n \psi_0;$$

however, for sake of definiteness we restrict our analysis to the Lie-type approximation method (31). The crucial point is to give a rigorous estimate of the remaining term

$$\mathcal{R}_n \psi_0 := S^{n\delta} \psi_0 - [X^\delta Y^\delta]^n \psi_0. \tag{32}$$

Typically one has that

$$\|\mathcal{R}_n \psi_0\|_{L^2} \leq C\delta \tag{33}$$

for some positive constant $C = C(\psi_0, t^*)$ independent of $n < t^*/\delta$. We should also mention that a purely formal (not completely rigorous) argument suggests that [30]

$$\|\mathcal{R}_n \psi_0\|_{L^2(\mathbb{R})} \leq C\delta^2 e^{C\delta}$$

for some positive constant $C = C(\psi_0, T)$, provided that the potential $V(x)$ is a bounded function and $\psi_0 \in H^2(\mathbb{R})$.

Data availability

All data generated or analysed during this study are included in this published article.

References

- [1] M.V. Berry, Quantal phase factors accompanying adiabatic changes, *Proc. R. Soc. Lond. Ser. A, Math. Phys. Sci.* 32 (1984) 45–57.
- [2] J.E. Avron, The lifetime of Wannier ladder states, *Ann. Phys. (NY)* 143 (1982) 33–53.
- [3] V. Grecchi, A. Sacchetti, Crossing and anticrossing of resonances: The Wannier-Stark ladders, *Ann. Phys. (NY)* 241 (1995) 258–284.
- [4] V. Grecchi, A. Martinez, A. Sacchetti, Double-well Stark effect: crossing and anticrossing of resonances, *Asympt. Anal.* 13 (1996) 373–391.
- [5] V. Grecchi, A. Martinez, A. Sacchetti, Splitting instability: the unstable double-wells, *J. Phys. A: Math. Gen.* 29 (1996) 4561–4587.
- [6] H.J. Korsch, S. Mossmann, Stark resonances for a double- δ quantum well: crossing scenarios, exceptional points and geometric phases, *J. Phys. A: Math. Gen.* 36 (2003) 2139–2153.
- [7] K. Datchev, N. Malawo, Semiclassical resonance asymptotics for the delta potential on the half line, *Proc. Amer. Math. Soc.* 150 (2022) 4909–4921.
- [8] S. Dyatlov, M. Zworski, *Mathematical Theory of Scattering Resonances*, in: AMS - Graduate Studies in Mathematics, vol. 200, 2019.
- [9] N. Moiseyev, Quantum theory of resonances: calculating energies, widths and cross-section by complex scaling, *Phys. Rep.* 302 (1998) 211–293.
- [10] K. Rapedius, Calculating resonance positions and widths using the siegert approximation method, *Eur. J. Phys.* 32 (2011) 1199–1211.
- [11] O. Rosas-Ortiz, N. Fernández-García, N. Cruz y Cruz, A primer on resonances in quantum mechanics, *AIP Conf. Proc.* 1077 (2008) 31–57.
- [12] A. Sacchetti, Double-barrier resonances and time decay of the survival probability: A toy model, in: A. Michelangeli, G. Dell’Antonio (Eds.), *Advances in Quantum Mechanics*, in: Springer INdAM Series, vol. 18, Springer, 2017, pp. 283–293.
- [13] A. Sacchetti, Tunnel effect and analysis of the survival amplitude in the nonlinear Winter’s model, *Ann. Phys. (NY)* 457 (2023) 169434:1-31.
- [14] B. Simon, Resonances in n -body quantum systems with dilatation analytic potentials and the foundations of time-dependent perturbation theory, *Ann. Math.* 97 (1973) 247–274.
- [15] B. Simon, Resonances and complex scaling: a rigorous overview, *Intl. J. Quant. Chem.* 14 (1978) 529–542.
- [16] G. García-Calderón, R. Peierls, Resonant states and their uses, *Nucl. Phys. A* 265 (1976) 443–460.
- [17] S. Albeverio, Høegh-Krohn R., The resonance expansion for the Green’s function of the Schrödinger and wave equations, in: S. Albeverio, L.S. Ferreira, L. Streit (Eds.), *Resonances — Models and Phenomena*, in: Lecture Notes in Physics, vol. 211, Springer, Berlin, 1984, pp. 105–127.
- [18] P. Facchi, S. Pascazio, Quantum zeno dynamics: mathematical and physical aspects, *J. Phys. A* 41 (2008) 493001:1-45.
- [19] S. Graffi, V. Grecchi, G. Jona-Lasinio, Tunneling instability via perturbation theory, *J. Phys. A: Math. Gen.* 17 (1984) 2935–2944.
- [20] G. Jona-Lasinio, F. Martinelli, E. Scoppola, New approach in the semi-classical limit of quantum mechanics. I. Multiple tunnelings in one dimension, *Comm. Math. Phys.* 80 (1981) 223–254.
- [21] A. Trenkwalder, G. Spagnoli, G. Semeghini, S. Coop, M. Landini, P. Castilho, L. Pezzé, G. Modugno, M. Inguscio, A. Smerzi, M. Fattori, Quantum phase transitions with parity-symmetry breaking and hysteresis, *Nat. Phys.* 12 (2016) 826–829.
- [22] A. Sacchetti, Resonances crossing and electric field quantum sensors, *Phys. Scr.* 99 (2024) 105124:1-8.
- [23] S. Albeverio, F. Gesztesy, R. Høegh-Krohn, H. Holden, *Solvable Models in Quantum Mechanics*, Springer, Berlin, 1988.
- [24] S. Fassari, I. Popov, F. Rinaldi, On the behaviour of the two-dimensional Hamiltonian $-\Delta + \lambda [\delta(\vec{x} + \vec{x}_0) + \delta(\vec{x} - \vec{x}_0)]$ as the distance between the two centres vanishes, *Phys. Scr.* 95 (2020) 5209:1-10.
- [25] P. Harrison, *Quantum Wells, Wires and Dots: Theoretical and Computational Physics of Semiconductor Nanostructures*, Wiley, 2005.
- [26] B. Helffer, J. Sjöstr, Puits multiples en limite semi-classique. II. Interaction moléculaire. Symétries. Perturbation, *Ann. de L’ I. H. P. Phys. Théorique* 42 (1985) 127–212.
- [27] B. Helffer, *Semi-Classical Analysis for the Schrödinger Operator and Applications*, in: Lecture Notes in Mathematics, vol. 1336, Springer Verlag, 1998.
- [28] S. Descombes, M. Schatzman, Strang’s formula for holomorphic semi-groups, *J. Math. Pures Appl.* 81 (2002) 93–114.
- [29] T. Jahnke, C. Lubich, Error bounds for exponential operator splittings, *BIT* 40 (2000) 735–744.
- [30] W. Auzinger, T. Kassebacher, O. Koch, M. Thalhammer, Adaptive splitting methods for nonlinear Schrödinger equations in the semiclassical regime, *Numer. Algorithms* 72 (2016) 1–35.